Available online at www.sciencedirect.com
SCIENCE DIRECT®
Journal of Solid State Chemistry 177 (2004) 3939–3943
JOURNAL OF SOLID STATE CHEMISTRY
www.elsevier.com/locate/jssc

Synthesis and structure of ternary transition-metal silicides $Zr_3Mn_4Si_6$ and $Hf_3Mn_4Si_6$

Andriy V. Tkachuk, Shane J. Crerar, Arthur Mar*

Department of Chemistry, University of Alberta, Edmonton, Alberta, Canada T6G 2G2

Received 14 May 2004; received in revised form 3 August 2004; accepted 8 August 2004
Available online 18 September 2004

Abstract

The isostructural ternary transition-metal silicides $Zr_3Mn_4Si_6$ and $Hf_3Mn_4Si_6$ can be prepared by direct reaction of the elemental components or by arc-melting. The single-crystal structure of $Zr_3Mn_4Si_6$ was determined by X-ray diffraction (Pearson symbol $tP104$, tetragonal, space group $P4_2/mbc$, $Z = 8$, $a = 17.1325(7)$ Å, $c = 5.1058(2)$ Å). $Zr_3Mn_4Si_6$ is isostructural to $Nb_3Fe_3CrSi_6$ and contains an essentially ordered arrangement of the transition-metal atoms. Square antiprismatic clusters with Zr and Mn atoms at the corners and Si atoms at the center share opposite faces to form one-dimensional columns $^1_\infty[Zr_{6/2}Mn_{2/2}Si]$ extending along the c direction. These columns occupy channels that are outlined by a framework of edge- and face-sharing $MnSi_6$ octahedra. The extensive metal-metal interactions in the structure are complemented by Si–Si bonding in the form of dumbbells, linear chains, and zigzag chains.

Keywords: Zirconium; Hafnium; Manganese; Silicide; Crystal structure

1. Introduction

A few quaternary silicides of composition $T_{\sim 3}T'_{\sim 3}CrSi_{\sim 6}$ (T = Ti, Nb; T' = Fe, Co, Ni) have been investigated as protective coatings for niobium alloys in high-temperature applications [1]. They adopt an apparently unique structure type, first found for $Nb_3Fe_3CrSi_6$, in which disorder can potentially arise between any combination of the transition-metal atoms [2]. It is unclear if the $Nb_3Fe_3CrSi_6$-type structure must be inherently disordered to be stable. The observation of a preferential occupation of the metal sites suggests that an ordered variant might be possible in the limiting extreme and that perhaps simpler ternary representatives with this structure type could be prepared.

In the (Zr, Hf)–Mn–Si systems, the phases ZrMnSi [3,4], $ZrMnSi_2$ [5], $Zr_{0.7}Si_{0.3}Mn_2$ [6], HfMnSi [3,4], and $HfMnSi_2$ [7] have been identified previously. We present here two silicides, $Zr_3Mn_4Si_6$ and $Hf_3Mn_4Si_6$, that are new ternary ordered representatives of the $Nb_3Fe_3CrSi_6$-type structure.

2. Experimental

2.1. Synthesis

$Zr_3Mn_4Si_6$ was first identified as a side product resulting from attack of the silica tube in a reaction intended for the preparation of Zr_5MnSb_2 in the presence of an Sn flux at 1000 °C. The small thin needle-shaped crystals of $Zr_3Mn_4Si_6$ were confirmed by energy-dispersive X-ray (EDX) analysis on a Hitachi S-2700 scanning electron microscope to contain 22% Zr, 35% Mn, and 43% Si (mol%), in good agreement with the expected values of 23% Zr, 31% Mn, and 46% Si, and with no other elements present. Subsequently, rational synthesis was carried out by direct reaction of stoichiometric mixtures of the elements (Zr, 99.7%,

*Corresponding author. Fax: +1-780-492-8231.
E-mail address: arthur.mar@ualberta.ca (A. Mar).

0022-4596/$ - see front matter © 2004 Elsevier Inc. All rights reserved.
doi:10.1016/j.jssc.2004.08.013

Cerac; Hf, 99.6%, Alfa-Aesar; Mn, 99.95%, Cerac; Si, 99.96%, Cerac) at 1000 °C for 2 weeks. The products were analyzed by X-ray powder diffraction on an Enraf-Nonius FR552 Guinier camera. The refined cell parameters are $a = 17.143(4)$ Å, $c = 5.115(2)$ Å, $V = 1503.2(7)$ Å^3 for $Zr_3Mn_4Si_6$ (in good agreement with the single-crystal cell parameters (vide infra)) and $a = 17.131(7)$ Å, $c = 5.105(3)$ Å, $V = 1498.2(9)$ Å^3 for $Hf_3Mn_4Si_6$. These phases can also be obtained by annealing ingots, which were prepared by arc melting in a Centorr 5TA tri-arc furnace, at 800 °C for 2 weeks. The cell parameters of the arc-melted products show some deviation suggesting that there is some degree of homogeneity, which may be related to partial disorder or nonstoichiometry in the transition-metal sites, or that longer annealing times may be required for full equilibration.

2.2. Structure determination

Intensity data were collected on a Bruker Platform/SMART 1000 CCD diffractometer at 22 °C using ω scans (0.2°) on a single crystal of $Zr_3Mn_4Si_6$ confirmed to contain all three elements by EDX analysis. Crystal data are given in Table 1. Calculations were carried out with use of the SHELXTL (version 5.1) package [8]. Face-indexed numerical absorption corrections were applied. The centrosymmetric space group $P4_2/mbc$ was chosen and initial atomic positions were found by direct methods. Refinements proceeded in a straightforward manner, but following the suggestion of a reviewer, we also examined the possibility of disorder within the transition-metal sites. Successive refinements were attempted in which each of these sites was allowed to be occupied by a mixture of Zr and Mn atoms. The occupancies converged to either 1.00(2) Zr or 1.00(2) Mn, with the exception of one site, labeled Zr3, where the occupancies were 0.88(2) Zr and 0.12 Mn, resulting in the formula $Zr_{2.88(2)}Mn_{4.12}Si_6$. An alternative possibility is that the structure is ordered but this site is deficient in Zr. A refinement along these lines led to an occupancy of 0.97(1) Zr, resulting in the essentially fully stoichiometric formula $Zr_{2.97(1)}Mn_4Si_6$. We do not consider determination of composition from refinement of X-ray diffraction data to be meaningful unless corroborated by other evidence. Both models are consistent with the EDX analysis and the variation in powder cell parameters. Examination of bond lengths argues for an ordered model, as the metal–Si distances to this site are too long to be consistent with occupation by Mn atoms. In the final refinement, we have accepted the ordered, fully stoichiometric model $Zr_3Mn_4Si_6$. The final difference electron density map is featureless. The atomic positions were standardized with the program STRUCTURE TIDY [9]. Note that this standardization changes some of the labels compared to the structure of $Nb_3Fe_3CrSi_6$ [2]. Final values of the positional and displacement parameters are given in Table 2. Interatomic distances are listed in Table 3. Further data, in the form of a CIF, have been sent to Fachinformationszentrum Karlsruhe, Abt. PROKA, 76344 Eggenstein-Leopoldshafen, Germany, as supplementary material No. CSD-414299 and can be obtained by contacting FIZ (quoting the article details and the corresponding CSD numbers).

Table 1
Crystallographic data for $Zr_3Mn_4Si_6$

Formula	$Zr_3Mn_4Si_6$
Formula mass (amu)	661.96
Space group	D_{4h}^{13}–$P4_2/mbc$ (No. 135)
a (Å)[a]	17.1325(7)
c (Å)[a]	5.1058(2)
V (Å^3)	1498.67(10)
Z	8
ρ_{calcd} (g cm^{-3})	5.868
Crystal dimensions (mm)	$0.40 \times 0.04 \times 0.03$
Radiation	Graphite monochromated Mo$K\alpha$, $\lambda = 0.71073$ Å
μ(Mo$K\alpha$) (cm^{-1})	113.97
Transmission factors	0.190–0.723
2θ limits	$3.36° \leqslant 2\theta$ (Mo$K\alpha$) $\leqslant 66.20°$
Data collected	$-25 \leqslant h \leqslant 25$, $-24 \leqslant k \leqslant 25$, $-7 \leqslant l \leqslant 7$
No. of data collected	17832
No. of unique data, including $F_o^2 < 0$	1535
No. of unique data, with $F_o^2 > 2\sigma(F_o^2)$	1446
No. of variables	75
$R(F)$ for $F_o^2 > 2\sigma(F_o^2)$ [b]	0.025
$R_w(F_o^2)$ [c]	0.057
Goodness of fit	1.229
$(\Delta\rho)_{max}, (\Delta\rho)_{min}$ (e Å^{-3})	1.19, −0.96

[a] Obtained from a refinement constrained so that $a = b$ and $\alpha = \beta = \gamma = 90°$.

[b] $R(F) = \sum||F_o| - |F_c||/\sum|F_o|$.

[c] $R_w(F_o^2) = \left[\sum[w(F_o^2 - F_c^2)^2]/\sum wF_o^4\right]^{1/2}$; $w^{-1} = [\sigma^2(F_o^2) + (0.0193p)^2 + 7.9862p]$, where $p = [\max(F_o^2, 0) + 2F_c^2]/3$.

3. Results and discussion

$Zr_3Mn_4Si_6$ and $Hf_3Mn_4Si_6$ are new phases in the (Zr, Hf)–Mn–Si systems. Although their composition is close to $ZrMnSi_2$ and $HfMnSi_2$, there is no simple relationship with these structures. Instead, they are isostructural with $Nb_3Fe_3CrSi_6$ [2], which has been previously described as an intergrowth of $Zr_4Co_4Ge_7$-type [10] and $Nb_2Cr_4Si_5$-type blocks [11]. The structure of $Zr_3Mn_4Si_6$, projected along the c direction, is shown as different representations in Fig. 1. The cluster description in Fig. 1(a) emphasizes the presence of Si-centered square antiprisms (made up of staggered pairs of squares with one Mn and three Zr atoms at the vertices) and $MnSi_6$ octahedra. The square antiprisms share opposite faces

Table 2
Atomic coordinates and equivalent isotropic displacement parameters for $Zr_3Mn_4Si_6$

Atom	Wyckoff position	x	y	z	U_{eq} (Å^2)[a]
Zr1	8*h*	0.20427(2)	0.10168(2)	0	0.00388(8)
Zr2	8*h*	0.28198(2)	0.29871(2)	0	0.00400(8)
Zr3	8*h*	0.47279(2)	0.20998(2)	0	0.00586(9)
Mn1	16*i*	0.05172(2)	0.15410(2)	0.24973(8)	0.00403(9)
Mn2	8*h*	0.38428(4)	0.04193(4)	0	0.00729(12)
Mn3	8*g*	0.62585(2)	0.12585(2)	$\frac{1}{4}$	0.00489(12)
Si1	8*h*	0.02157(7)	0.43451(7)	0	0.0079(2)
Si2	8*h*	0.06132(7)	0.03048(7)	0	0.0087(2)
Si3	8*h*	0.13082(6)	0.24753(6)	0	0.0049(2)
Si4	8*h*	0.22549(6)	0.45254(6)	0	0.0054(2)
Si5	8*h*	0.43028(7)	0.36132(6)	0	0.0053(2)
Si6	8*g*	0.16235(4)	0.66235(4)	$\frac{1}{4}$	0.0046(2)

[a] U_{eq} is defined as one-third of the trace of the orthogonalized U_{ij} tensor.

Table 3
Selected interatomic distances (Å) for $Zr_3Mn_4Si_6$

Zr1–Si2	2.7361(12)	Mn1–Si4	2.4278(10)
Zr1–Si3	2.7978(12)	Mn1–Si5	2.4375(10)
Zr1–Si6	2.8163(5) (× 2)	Mn1–Si3	2.4545(10)
Zr1–Si4	2.8243(12)	Mn1–Si5	2.4546(10)
Zr1–Si5	2.8425(5) (× 2)	Mn1–Si2	2.4775(11)
Zr1–Mn1	3.0434(5) (× 2)	Mn1–Si2	2.4785(11)
Zr1–Mn1	3.0462(5) (× 2)	Mn1–Mn1	2.5502(8)
Zr1–Mn2	3.2494(7)	Mn1–Mn1	2.5556(8)
Zr1–Zr3	3.2099(3) (× 2)	Mn1–Zr3	2.9796(5)
Zr1–Zr2	3.2392(3) (× 2)	Mn1–Zr1	3.0434(5)
		Mn1–Zr1	3.0462(5)
Zr2–Si3	2.7342(11)	Mn1–Zr2	3.0656(5)
Zr2–Si5	2.7578(12)		
Zr2–Si4	2.8076(12)	Mn2–Si1	2.3866(13)
Zr2–Si6	2.8280(10) (× 2)	Mn2–Si4	2.4252(13)
Zr2–Si3	2.8689(5) (× 2)	Mn2–Si1	2.4473(13)
Zr2–Mn1	3.0656(5) (× 2)	Mn2–Si6	2.5541(10) (× 2)
Zr2–Mn3	3.2334(6) (× 2)	Mn2–Si1	2.9054(6) (× 2)
Zr2–Zr2	3.2156(4) (× 2)	Mn2–Mn2	3.1168(7) (× 2)
Zr2–Zr1	3.2392(3) (× 2)	Mn2–Mn3	3.1499(7) (× 2)
		Mn2–Zr3	3.0312(4) (× 2)
Zr3–Si1	2.6126(13)	Mn2–Zr1	3.2494(7)
Zr3–Si5	2.6933(12)	Mn2–Zr3	3.2541(8)
Zr3–Si6	2.7669(5) (× 2)		
Zr3–Si3	2.8035(12)	Mn3–Si1	2.4269(11) (× 2)
Zr3–Si4	2.8678(5) (× 2)	Mn3–Si3	2.5185(10) (× 2)
Zr3–Mn1	2.9796(5) (× 2)	Mn3–Si4	2.5194(10) (× 2)
Zr3–Mn2	3.0312(4) (× 2)	Mn3–Mn3	2.55290(11) (× 2)
Zr3–Mn3	3.2531(4) (× 2)	Mn3–Mn2	3.1499(7) (× 2)
Zr3–Mn2	3.2541(8)	Mn3–Zr2	3.2334(6) (× 2)
Zr3–Zr1	3.2099(3) (× 2)	Mn3–Zr3	3.2531(4) (× 2)
Si1–Si1	2.363(2)	Si2–Si2	2.346(2)
Si1–Si1	2.7658(9) (× 2)	Si6–Si6	2.55290(11) (× 2)

and extend along the *c* direction to form one-dimensional columns. Tetrameric groups of edge-sharing Mn1-centered octahedra are connected together via Mn3-centered octahedra; these octahedra share faces along the *c* direction to form a channel framework within which the square antiprismatic clusters lie. The description in Fig. 1(b) illustrates how the structure can also be built up by stacking two-dimensional nets. The primary layers A and A' lying at $z = 0$ and $\frac{1}{2}$, respectively, are related by a fourfold screw operation and are constructed from a tessellation of triangles, squares, pentagons, and hexagons. The remaining atoms lie in secondary layers at $z = \sim \frac{1}{4}$ or $z = \sim \frac{3}{4}$.

The three Zr sites at the corners of the square antiprisms are coordinated to seven Si atoms at 2.6126(13)–2.8689(5) Å in a pentagonal bipyramidal geometry. The fourth site, occupied by Mn, is coordinated to five Si atoms at 2.3866(13)–2.5541(10) Å in a distorted trigonal bipyramidal geometry and two further Si atoms at 2.9054(6) Å. These distances are similar to those found in $ZrMnSi_2$ [5]. Interatomic distances between metal atoms (Zr–Zr, 3.2099(3)–3.2392(3) Å; Zr–Mn, 2.9796(5)–3.2541(8) Å; Mn–Mn, 2.5502(8)–3.1499(7) Å) are consistent with the sum of the metallic radii (Zr, 1.60 Å; Mn, 1.27 Å) [12]. As shown in Fig. 2, significant Si–Si interactions persist in this metal-rich structure within the Si_2 dumbbells (Si1–Si1, 2.363(2) Å; Si2–Si2, 2.346(2) Å) straddling pairs of $MnSi_6$ octahedra, the linear Si chains (Si6–Si6, 2.55290(11) Å, corresponding to half the *c* parameter) forming the spine of the $^1_\infty[Zr_{6/2}Mn_{2/2}Si]$ columns, and possibly the zigzag Si chains (Si1–Si1, 2.7658(9) Å) associated with face-sharing Mn3-centered octahedra. Si–Si distances as long as 2.8 Å have been implicated as non-innocent, and overlap populations within a linear Si chain in $Zr_2Cr_4Si_5$ can be nearly as large as within a Si_2 dumbbell [13].

The ordered distribution of the metal atoms in $Zr_3Mn_4Si_6$, in contrast to that in $Nb_3Fe_3CrSi_6$, can be attributed to more pronounced size differences (Zr/Mn vs. Nb/(Fe, Cr)). Any of the octahedral sites should be suitable for occupation by Cr, Mn, or Fe, which have nearly identical metallic radii (1.28–1.26 Å) [12]. In $Nb_3Fe_3CrSi_6$, two of the sites forming the corners of the

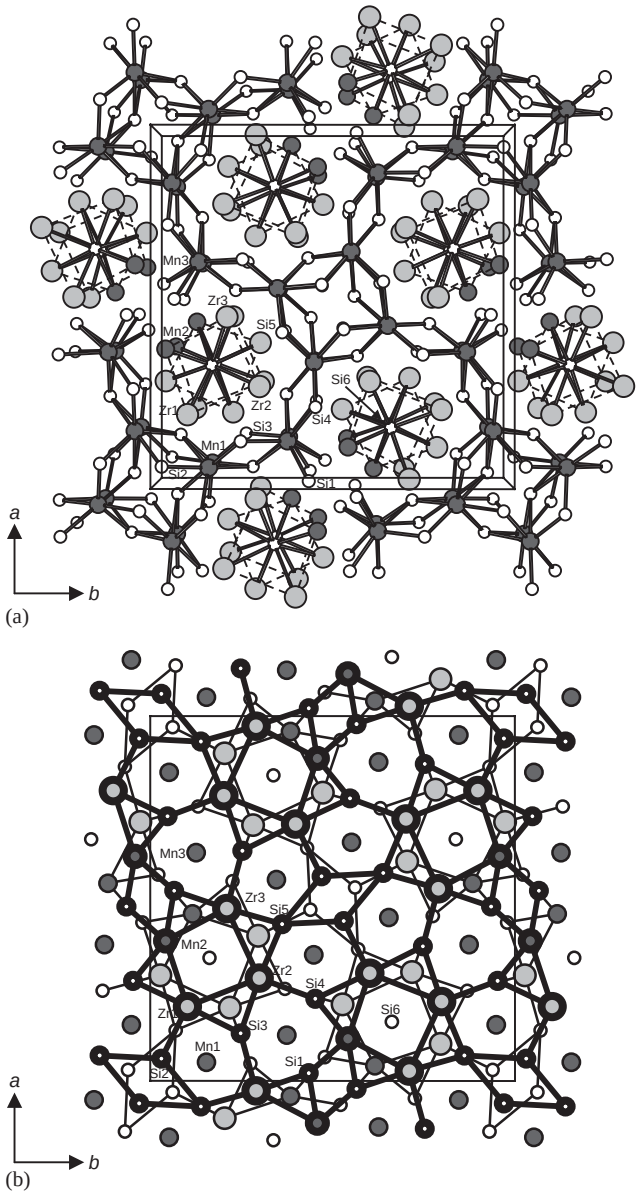

Fig. 1. Projection down the c-axis of the structure of $Zr_3Mn_4Si_6$, in terms of (a) Si-centered square antiprisms and Mn-centered octahedra, or (b) stacking of two-dimensional nets at $z=0$ (thick lines) and $z=\frac{1}{2}$ (thin lines) with remaining atoms in secondary layers at $z=\sim\frac{1}{4}$ or $z=\sim\frac{3}{4}$. The large lightly shaded circles are Zr atoms, the medium solid circles are Mn atoms, and the small open circles are Si atoms.

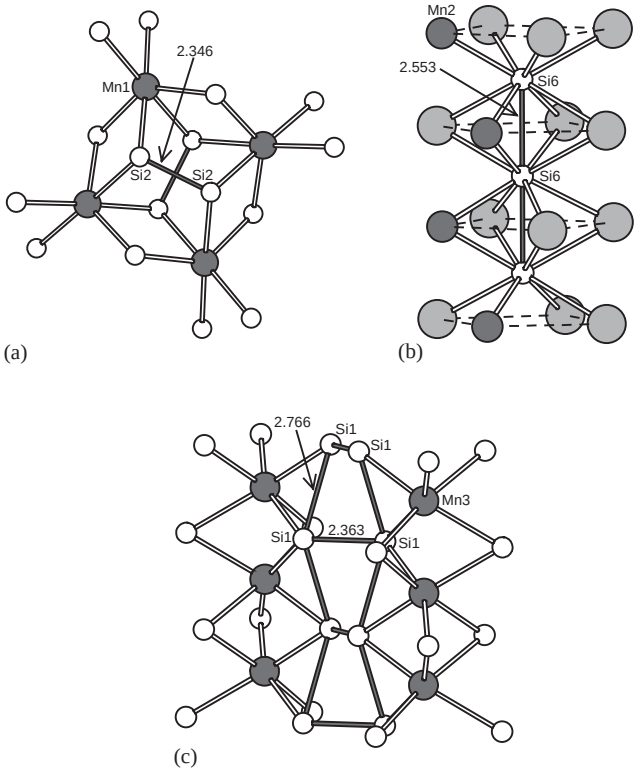

Fig. 2. Important Si–Si interactions (Å) in $Zr_3Mn_4Si_6$ in the form of Si_2 dumbbells, linear Si chains, and zigzag Si chains.

square antiprisms are disordered (with occupancies of 0.42(12) Cr, 0.58(12) Fe and 0.12(2) Cr, 0.88(2) Nb, respectively) [2]. In $Zr_3Mn_4Si_6$, these sites (Mn2 and Zr3) appear to be completely ordered. The possibility that the Zr3 site is disordered with a small amount of Mn is unlikely as all distances from this site to the Si atoms significantly exceed the normal Mn–Si bond length of 2.4–2.5 Å. A more feasible possibility is that the Zr3 site can be slightly deficient, leading to some degree of homogeneity and accounting for the variability in cell parameters depending on the method of preparation. This structure type seems to be quite flexible in terms of its electron count and it should be possible to substitute Mn with other transition metals in $Zr_3Mn_4Si_6$ and $Hf_3Mn_4Si_6$ to generate other members of this series.

Acknowledgments

The Natural Sciences and Engineering Research Council of Canada and the University of Alberta supported this work. We thank Dr. Robert McDonald (Faculty Service Officer, X-ray Crystallography Laboratory) for the X-ray data collection and Ms. Christina Barker (Department of Chemical and Materials Engineering) for assistance with the EDX analysis.

References

[1] M. Vilasi, M. François, R. Podor, J. Steinmetz, J. Alloys Compd. 264 (1998) 244.
[2] M. Vilasi, G. Venturini, J. Steinmetz, B. Malaman, J. Alloys Compd. 194 (1993) 127.
[3] Ya.P. Yarmolyuk, A.K. Shurin, E.I. Gladyshevskii, Dopov. Akad. Nauk Ukr. RSR Ser. A: Fiz.-Tekh. Mat. Nauki 32 (1970) 558.
[4] W. Bażela, A. Szytuła, J. Leciejewicz, Phys. Status Solidi A 94 (1986) 207.

[5] G. Venturini, J. Steinmetz, B. Roques, J. Less-Common Met. 87 (1982) 21.
[6] Ž. Blažina, R. Trojko, J. Less-Common Met. 133 (1987) 277.
[7] Ya.P. Yarmolyuk, M. Sikiritsa, L.G. Aksel'rud, L.A. Lysenko, E.I. Gladyshevskii, Sov. Phys. Crystallogr. (Engl. Transl.) 27 (1982) 652.
[8] G.M. Sheldrick, SHELXTL, Version 5.10, Bruker AXS Inc., Madison, WI, 1998.
[9] L.M. Gelato, E. Parthé, J. Appl. Crystallogr. 20 (1987) 139.
[10] W. Jeitschko, Acta Crystallogr. Sect. B: Struct. Crystallogr. Cryst. Chem. 25 (1969) 557.
[11] P.I. Kripyakevich, Ya.P. Yarmolyuk, E.I. Gladyshevskii, Sov. Phys. Crystallogr. (Engl. Transl.) 13 (1969) 677.
[12] L. Pauling, The Nature of the Chemical Bond, 3rd ed, Cornell University Press, Ithaca, NY, 1960.
[13] S.J. Crerar, A. Mar, J. Solid State Chem. 177 (2004) 2523.